Polyelectrolyte Brush Density Profiles

F. von Goeler and M. Muthukumar*

Department of Physics and Astronomy and Polymer Science and Engineering Department, University of Massachusetts, Amherst, Massachusetts 01003

Received January 31, 1995; Revised Manuscript Received April 21, 1995[⊗]

ABSTRACT: A study of the density profile of polyelectrolyte brushes in electrolyte solutions is presented. We consider a monomer–monomer potential with two components: (1) a short-ranged excluded volume component with strength $\bar{w}l^3$ (l is the Kuhn length) and (2) a screened Coulombic long-ranged component with strength $\bar{v}/l$ and range κ^{-1}. We examine the dependence of brush height, d, with polyelectrolyte chain length L ($=lN$), grafting density, σ, and κ. The dimensionless variables are $wN^{3/2}$, $vN^{5/2}$, and $\kappa lN^{1/2}$, where $v = 2\pi\sigma\bar{v}l^2$, and $w = \bar{w}\sigma l^2$. Dimensional analysis, computational enumeration, and a variational procedure are used to obtain the characteristics of the density profile. Four regimes of electrostatic interaction are identified: (1) a weak interaction regime in which $d \sim L^\nu$ with an effective ν between $^1/_2$ and $^3/_5$ depending on $wN^{3/2}$; (2) an intermediate regime for intermediate values of $vN^{5/2}$ where the scaling $d \sim vN^3$ is possible if $\kappa lN^{1/2}$ is small; (3) a regime where both $\kappa lN^{1/2}$ and $vN^{5/2}$ are large where the electrostatic interaction is essentially short-ranged due to screening and $d \sim (w + (2v/\kappa^2l^2)^{1/3}lN$; and (4) a fully stretched (saturation) regime where $d \approx lN$ due to finite extensibility of the chains. The various crossover behaviors between these asymptotic regions are also obtained with quantitative details.

I. Introduction

Polyelectrolyte brushes consist of electrically charged polymer chains which are terminally grafted to a surface. When the chains are in a salt solution, the electrical repulsion between monomers on the chain is screened by counterions and the dissociated ions of the salt. Therefore, the salt concentration in the solution controls the size of a polyelectrolyte brush: when the salt concentration is low, the effect of screening is weak and the size of the brush is large compared with the size of the brush in a high concentration of salt. An understanding of polyelectrolyte brushes is essential in the area of colloid stabilization[1] and some biologically important systems.[2]

Uncharged polymer brushes are well understood because of a great deal of theoretical,[3–12] computational,[13,14] and experimental[15–20] work (refs 19 and 20 review much of this work). Dolan and Edwards[3] have calculated the force between two brush surfaces containing Gaussian (noninteracting) chains. From scaling arguments, Alexander[5] and de Gennes[4] have determined the following relationships between brush height, d, and the polymer length, L ($=lN$), where N is the number of Kuhn segments and l is the segment length, for the case of self-excluding polymers in a solvent with a bulk scaling exponent ν. The exponent ν describes the scaling of the radius of gyration, R_g, with N (i.e. $R_g \sim N^\nu$); ν is $^3/_5$ in a good solvent and $^1/_2$ in a Θ solvent. The theory of Alexander and de Gennes makes the following predictions: if the average distance between graft points is large compared with size of the polymer R_g in the bulk, then $d \sim lN^\nu$; if the average distance between grafts is small compared with the size of the polymer in the bulk, then $d \sim (\sigma l^2)^{(1-\nu)/2\nu}Nl$, where σ is the grafting density per surface area. The latter result corresponds to a strong stretching regime for the excluded volume brush. Milner *et al.*[6] and Zhulina *et al.*[7] consider a brush with a high grafting density and a short-range, self-excluding interaction by analogy between the mean field free energy of the brush and the classical path of a particle in a potential field. In contrast with scaling theory, which assumes a step-function density profile, this approach predicts a parabolic density profile for the self-excluding brush. Muthukumar and Ho[8] use a self-consistent field technique to determine the density profile of self-excluding brushes. Carignano and Szleifer have computed the probability distribution function of the grafted chain conformation by assuming an incompressible polymer/solvent system.[11] This procedure gives density profiles which are equivalent to those obtained by the self-consistent field technique. The results of these works indicate a density profile which is roughly parabolic for strongly self-excluding brushes but with a zero density at the surface and an exponentially decaying tail. Density profiles with these features have also been observed in simulations using molecular dynamics and Monte Carlo algorithms.[13,14] Force measurements between surfaces with adsorbed block copolymers are consistent with the scaling theory model but cannot determine the form of the density profile exactly.[17] Neutron scattering measurements using polystyrene brushes indicate a density profile which is parabolic with a small exponential tail.[18]

Recently, the problem of polyelectrolyte brushes was considered by several investigators.[21–27] Because of the nature of the long-range monomer–monomer potential, this problem is more difficult to treat theoretically than that of the self-excluding brush. Pincus considers a step-function density profile and uses scaling arguments similar to those of Alexander and de Gennes to determine the relationship between the brush height, d, length (i.e. molecular weight), L, grafting density, σ, and linear charge density, q, along the chain.[23,24] Using a linearized Poisson–Boltzmann distribution of counterions, this approach determines the brush height by balancing the osmotic pressure of counterions with the effective force due to the entropy of the brush. Two cases are considered: (1) a no salt regime in which $d \approx 2\pi\sigma e^2q^2N^3l^4/\epsilon k_BT$ if the screening length, κ^{-1}, due to counterions is large compared with d, and $d \sim q^{1/2}l^{3/2}N$ if $\kappa^{-1} \leq d$; (2) a high salt concentration regime (i.e. strong screening case) where $d \approx (\sigma/2lc_s)^{1/3}lN$. Here, ϵ is the dielectric constant of the solution, k_BT is Boltzmann's constant times the absolute temperature, and c_s is the salt concentration. Similar results were obtained by Borisov, Birshtein, and Zhulina who, in

[⊗] Abstract published in *Advance ACS Abstracts,* August 1, 1995.

0024-9297/95/2228-6608$09.00/0

addition, considered the collapse of grafted polyelectrolyte layers.[25-27] These authors obtained scaling laws by analyzing asymptotic solutions of the Poisson–Boltzmann equation at arbitrary grafting and charge density including the regime of nonoverlapped grafted polyions.

While an analytical solution for charged polymer brushes using the mean-field approach of Zhulina *et al.*[7] and Milner *et al.*[6] does not seem possible, Miklavic and Marcelja[21] and Misra, Varanasi, and Varanasi[22] have treated this problem numerically. As in the case of a self-excluding short-range potential, this work predicts a roughly parabolic density profile which becomes extended with increasing charge density or decreasing salt concentration. Although, in principle, the application of the self-consistent procedure of Muthukumar and Ho to this problem is straightforward, there are difficulties associated with the stability of numerical solutions of the necessary differential equations.

In the present work, the density profile of a polyelectrolyte brush is studied through the use of computational enumeration. The results are compared with a variational calculation. This numerical approach overcomes difficulties associated with the self-consistent method and includes the effect of fluctuations which are neglected in mean-field approximations of the density profile. This paper presents a study of the polyelectrolyte brush problem which analyzes in detail the density profile and effects of molecular weight, polyelectrolyte charge density, and salt concentration in solution. The self-consistent field procedure used in the present work allows us to consider only the case of high grafting density (i.e. "brush" regime). The regime of nonoverlapped grafted polyions (i.e. "mushroom" regime) addressed in refs 25–27 is not contained in the present work.

The outline of this paper is as follows. In section II, the polyelectrolyte brush is modeled. A scaling analysis of relevant variables is given in section III. Section IV describes a computational enumeration for the problem of the polyelectrolyte brush in addition to considering the case of a short-ranged, self-excluding potential. A variational procedure is used to predict the crossover behavior of the brush in section V. Section VI consists of a summary of this work and a discussion of the results.

This work shows that for a brush of polyelectrolytes of chain length, L, with only a screened Coulombic interaction (without the usual short-ranged van der Waals interaction between segments) of strength v and range κ^{-1}, the height, d, of the brush depends only upon the variables $vN^{5/2}$ and $\kappa lN^{1/2}$. Here, $v = 2\pi\sigma q^2 e^2 l^3/\epsilon k_B T$ where q is the number of charges per Kuhn length and κ^{-1} is the Debye screening length associated with dissociated salt ions and counterions of the polyelectrolyte in solution. At very low values of $vN^{5/2}$, the brush height is proportional to $N^{1/2}$, corresponding to a Gaussian brush. At intermediate values of $vN^{5/2}$, the brush height is also proportional to $N^{1/2}$ if $\kappa lN^{1/2}$ is sufficiently large. At intermediate values of $vN^{5/2}$, if $\kappa lN^{1/2}$ is small, the brush height is proportional to vlN^3. When both $vN^{5/2}$ and $\kappa lN^{1/2}$ are large, the brush height, d, depends upon a single variable, $vN^{3/2}/\kappa^2 l^2$ ($=vN^{5/2}/(\kappa lN^{1/2})^2$): if this variable is small, then the screening dominates and the brush is Gaussian with $d \sim lN^{1/2}$; if this variable is large, then the electrostatic interaction is effectively short-ranged with strength $2v/\kappa^2 l^2$ and the brush size is proportional to $v^{1/3}\kappa^{-2/3}l^{1/3}N$. Finally, because of finite extensibility, for strongly stretched brushes, there is a saturation regime where $d \approx lN$.

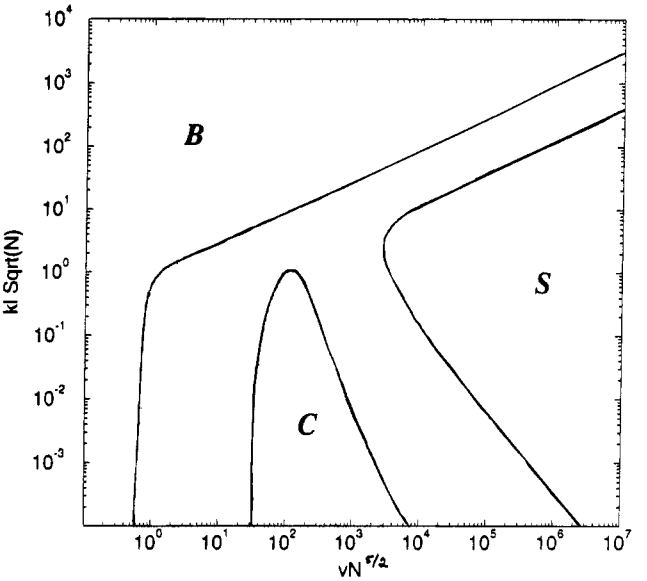

Figure 1. Summary of the results with quantitative details from variational and enumeration calculations.

These results are only asymptotic results. We have calculated the range of the two dimensionless variables, $vN^{5/2}$ and $\kappa lN^{1/2}$, where the above asymptotic results are valid. We have also obtained explicitly the crossover behavior between these two regimes. All of the conclusions are presented quantitatively in Figure 1, where $vN^{5/2}$ and $\kappa lN^{1/2}$ are plotted on the abscissa and ordinate, respectively. In the region designated B, $d \sim N^{\nu}$ with $\nu = {}^1/_2$. When the usual short-ranged van der Waals excluded volume interaction is considered, as is shown in the following sections, $\nu = {}^3/_5$ in the region B. The region designated S corresponds to the situation $d \sim v^{1/3}\kappa^{-2/3}l^{1/3}N$. The region labeled C shows the intermediate values of $vN^{5/2}$ where $d \sim vN^3$. In fact, region C is itself a crossover region. The effective exponent α for the N-dependence of d, $d \sim N^{\alpha}$, changes smoothly from 3 at very low values of $\kappa lN^{1/2}$ to 1 and eventually to ${}^1/_2$ as $\kappa lN^{1/2}$ is increased continuously. The unmarked regions in Figure 1 are the various crossover regions between B, C, and S regimes. These crossover behaviors are discussed below. The saturation regime, FS, corresponding to the fully stretched chain due to finite extensibility, although discussed below, is not shown explicitly in Figure 1.

II. Model

A sketch of a typical brush of polyelectrolyte chains of contour length lN is shown in Figure 2. The case of a planar, uncharged grafting surface is considered. The number of charges per unit contour length, q, on the polyelectrolyte chain is uniform. A uniform grafting density, σ (i.e. number of polyelectrolyte chains per unit area of surface), is considered. A Cartesian coordinate system with the grafting surface defined by $z = 0$ is chosen; the z axis is perpendicular to the surface; the x and y axes are parallel to the surface. The brush height is d, and l is the segment length.

The monomer–monomer interaction considered has two parts: the familiar short-ranged excluded volume component of strength $\bar{v}l$ and a screened Coulombic electrostatic component of strength $\bar{v}/l = q^2e^2/\epsilon k_B T$ and range κ^{-1}. The inverse Debye length, κ^{-1}, is given by the Debye–Hückel linearized Poisson–Boltzmann theory:

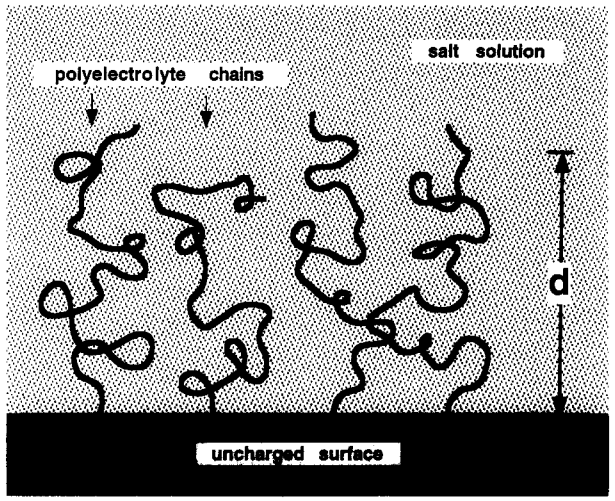

Figure 2. Anatomy of a polyelectrolyte brush.

$$\kappa^2 = \frac{4\pi e^2}{\epsilon k_B T}\sum_i n_i Z_i^2 \tag{2.1}$$

Here, e is the electronic charge, n_i and Z_i are the solution concentration and valence of the ith ionic species, and ϵ is the dielectric constant of the solution. This form is a reasonable approximation of the electrostatic interaction when the local charge density is not great and the screening length is large compared with the size of the salt ions in solution.

This problem is formulated mathematically by representing the ith polyelectrolyte chain as a continuous curve, $\mathbf{R}_i(s)$, which describes the position of the continuous arc-length parameter s ($0 \le s \le L$). The connectivity and intersegment interactions for a given configuration of chains, $\{\mathbf{R}_i(s)\}$, are described by the Edwards Hamiltonian:[28]

$$H[\{\mathbf{R}_i\}] = \frac{3}{2l}\sum_i \int_0^L ds \left\{\frac{\partial \mathbf{R}_i(s)}{\partial s}\right\}^2 + \frac{1}{2}\sum_i\sum_j \int_0^L ds \int_0^L ds'\, V[\mathbf{R}_i(s) - \mathbf{R}_j(s')] \tag{2.2}$$

with

$$V[\mathbf{R}_i(s) - \mathbf{R}_j(s')] = \bar{w} l \delta(\mathbf{R}_i(s) - \mathbf{R}_j(s')) + \frac{\bar{v}}{l}\frac{\exp(-\kappa|\mathbf{R}_i(s) - \mathbf{R}_j(s')|)}{|\mathbf{R}_i(s) - \mathbf{R}_j(s')|} \tag{2.2a}$$

In eq 2.2a, $\bar{w}l^3$ is the familiar short-ranged excluded volume parameter and $\bar{v}$ is the long-ranged electrostatic interaction parameter, $\bar{v} = q^2e^2l/\epsilon k_B T$.

The Boltzmann probability of a given configuration $\{\mathbf{R}_i\}$ is

$$P[\{\mathbf{R}_i\}] = Z^{-1}\, e^{-H[\{\mathbf{R}_i\}]} \tag{2.3}$$

where

$$Z \equiv \int D[\{\mathbf{R}_i(s)\}]\, e^{-H[\{\mathbf{R}_i\}]} \tag{2.3a}$$

For brushes, there is the obvious condition that the grafting point of each chain, $\mathbf{R}_i(s=0)$, is fixed and on the surface. The appropriate absorbing boundary condition for this problem is that all chains are restricted to the region $z > 0$. The integral in the denominator of eq 2.3 is, therefore, a functional integral over all sets of chains with $z_i(s) > 0$ for $0 < s \le L$ and with fixed grafting points at the surface. Using the probability given by eq 2.3, the density profile of the brush is

$$\langle \varrho(\mathbf{r})\rangle = Z^{-1}\int D[\{\mathbf{R}_i(s)\}]\sum_i \int_0^L ds\, \delta(\mathbf{R}_i(s) - \mathbf{r})\, e^{-H[\{\mathbf{R}_i\}]} \tag{2.4}$$

Using a discretized version of eq 2.4, the density profile of polyelectrolyte brushes can, in principle, be determined by enumeration on a computer. This approach, however, is prohibitively time consuming. Because only density variations in the direction perpendicular to the surface are of interest, and in order to make the problem tractable, an approximation is used: a uniform density distribution in planes parallel to the surface is assumed. With this simplification, an equivalent one-dimensional problem is considered with a one-dimensional screened Coulombic potential which may be determined by integration over planes of uniform charge. The screened Coulombic potential due to a uniformly charged planar surface is given in refs 29 and 30, for example. Therefore, the following Hamiltonian is used:

$$H[z(s)] = \frac{1}{2l}\int_0^L ds \left\{\frac{\partial z(s)}{\partial s}\right\}^2 + \frac{1}{2}\int_0^L ds \int_0^L ds'\, V[z(s) - z(s')] \tag{2.5}$$

with

$$V[z - z'] = \frac{w}{l}\delta(z - z') + \frac{v}{\kappa l^3}\exp(-\kappa|z - z'|) \tag{2.5a}$$

Here, v is proportional to the grafting density, σ. Specifically, $v = 2\pi\sigma q^2 e^2 l^3/\epsilon k_B T$ and $w = \bar{w}\sigma l^2$. The density is given by

$$\langle \varrho(z)\rangle = Z^{-1}\int D[z(s)]\int_0^L ds\, \delta(z(s) - z)\, e^{-H[\{\mathbf{R}_i\}]} \tag{2.6}$$

where now the partition function is

$$Z^{-1} \equiv \int D[z(s)]\, e^{-H[z(s)]} \tag{2.6a}$$

The assumption of uniform charge density in planes parallel to the grafting surface is valid for brushes with sufficiently large grafting densities; this approximation breaks down when the mean spacing between graft sites is greater than the height of the brush. This assumption is implicit in the theories discussed in the Introduction. Additionally, these theories make the mean-field approximation of considering only the minimum free energy distribution in the z direction. Section IV will describe a computation enumeration which avoids this approximation. Before this is considered, the scaling of the one-dimensional Hamiltonian (eq 2.5) will be analyzed.

III. Scaling Analysis

This section describes the scaling behavior of polyelectrolyte brushes with the effective Hamiltonian described by eq 2.5. When the variables s and z are made dimensionless through the use of Kuhn length, l, the Edwards Hamiltonian of eq 2.5 becomes

$$H(N,w,v,\kappa l) = \frac{1}{2}\int_0^N ds \left(\frac{\partial z_s}{\partial s}\right)^2 + \frac{1}{2}\int_0^N ds \int_0^N ds' \left(w\delta[z(s) - z(s')] + \frac{v}{\kappa l}\exp(-\kappa l|z(s) - z(s')|)\right) \quad (3.1)$$

Performing the scale transformations $as \rightarrow s$ and $a^{1/2}z \rightarrow z$, where $a > 0$ is arbitrary, yields

$$H(aN,wa^{-3/2},va^{-5/2},\kappa l a^{-1/2}) = \frac{1}{2}\int_0^{aN} ds \left(\frac{\partial z_s}{\partial s}\right)^2 + \frac{1}{2}\int_0^{aN} ds \int_0^{aN} ds' \left(wa^{-3/2}\delta[z(s) - z(s')] + \frac{va^{-5/2}}{\kappa l a^{-1/2}}\exp(-\kappa l a^{-1/2}|z(s) - z(s')|)\right) \quad (3.2)$$

The relevant dimensionless variables are obtained by choosing the arbitrary scaling variable a to be $1/N$ so that

$$H(N,w,v,\kappa l) = H(1,wN^{3/2},vN^{5/2},\kappa l N^{1/2}) \quad (3.3)$$

Therefore, the dimensionless variables are $wN^{3/2}$, $vN^{5/2}$, and $\kappa l N^{1/2}$.

When only the electrostatic interaction is present ($w = 0$), there are two independent variables describing the long-ranged electrostatic interaction, $vN^{5/2}$ and $\kappa l N^{1/2}$:

$$H = H[vN^{5/2},\kappa l N^{1/2}] \quad (3.4)$$

The brush height dependence upon these variables (when $w = 0$) should be of the form

$$d = lN^{1/2} f(vN^{5/2},\kappa l N^{1/2}) \quad (3.5)$$

If the charge density on the chains is small, corresponding to small $vN^{5/2}$, or the screening of the electrostatic interaction by ions in solution is strong, corresponding to large values of $\kappa l N^{1/2}$, then only entropy is important. The chain length dependence of the brush height, d, in this regime of small κ is obtained by the usual Flory-like argument from eq 3.1. Approximating $\exp(-\kappa l|z(s) - z(s')|)$ for small values of κl, dimensional analysis of eq 3.1 yields the "Flory free energy":

$$F = \frac{d^2}{N} + \frac{vN^2}{\kappa l}(1 - \kappa l d) \quad (3.6)$$

Minimization of F with respect to d gives the scaling

$$d \sim vN^3 \quad (3.7)$$

which is valid in the small κ limit when v is sufficiently large. Prefactors are completely ignored in getting this qualitative result. This scaling behavior was predicted by Pincus[23] for the "no salt" case when $\kappa^{-1} > lN$. Here, we find that $d \sim lN^3$ when $\kappa^{-1} > lN^{1/2}$.

A third regime of strong electrostatic screening exists in which the electrostatic interaction is essentially short-ranged. When κ is sufficiently large, we get from eq 2.2a

$$V[\mathbf{R}(s) - \mathbf{R}(s')] = \left(\bar{w}l + \frac{4\pi\bar{v}}{\kappa^2 l}\right)\delta[\mathbf{R}(s) - \mathbf{R}(s')] \quad (3.8)$$

Therefore the electrostatic interaction simply increases the strength of the short-ranged excluded volume interaction. The effective Hamiltonian is obtained by integrating out directions parallel with the surface,

$$H[z(s)] = \frac{1}{2l}\int_0^L ds \left(\frac{\partial z(s)}{\partial s}\right)^2 + \int_0^L ds \int_0^L ds' \left(\frac{w}{l} + \frac{2v}{\kappa^2 l^3}\right)\delta(z(s) - z(s')) \quad (3.9)$$

Dimensional analysis of eq 3.11 gives

$$F = \frac{d^2}{l^2 N} + \left(\frac{w}{l} + \frac{2v}{\kappa^2 l^3}\right)\frac{l^2N^2}{d} \quad (3.10)$$

Minimization of F with respect to d gives the scaling

$$d \sim \left(w + \frac{2v}{\kappa^2 l^2}\right)^{1/3} lN \quad (3.11)$$

When $w = 0$, $d \sim (v/\kappa^2 l^2)^{1/3} Nl$. In this regime, the brush height is proportional to the chain length. This behavior is equivalent to the self-avoiding walk statistics in one dimension.

A fourth regime corresponds to the case when the brush is fully stretched. This regime is indicated by the discretized version of eq 2.5. Because real brushes are only finitely extensible, at very high charge densities and long screening lengths, the brush height is given by

$$d \approx lN \quad (3.12)$$

Summarizing the scaling analysis for the case of electrostatic interaction, there are four regimes: (1) a *weak regime* realized by small v and large κ, with $d \sim lN^{1/2}$; (2) an *intermediate regime* of $\kappa^{-1} > lN^{1/2}$ where $d \sim vN^3$; (3) chain stretching due to the short-ranged excluded volume for large values of κ and sufficiently large values of v, $d \sim (v/\kappa^2 l^2)^{1/3} lN$; and (4) a *strong interaction regime* with full chain stretching, $d \approx lN$.

A similar analysis of the effect of the short-ranged excluded volume interaction indicates three regimes when $v = 0$: (1) a *weak interaction regime* at low values of $wN^{3/2}$; (2) chain stretching due to the excluded volume with $d \sim w^{1/3} lN$; and (3) a *strong interaction regime* at large values of $wN^{3/2}$ where the brush is fully stretched and $d \approx lN$.

When both v and w are not equal to zero, there are many crossover behaviors. When electrostatic interaction is present, the intermediate regime of $d \sim vN^3$ for $\kappa^{-1} > lN^{1/2}$ is between the three-dimensional excluded volume regime ($d \sim N^{3/5}$) and the one-dimensional excluded volume regime ($d \sim (w + (2v/\kappa^2 l^2)^{1/3})lN$). A higher value of about 3 may be realized for the effective exponent α ($d \sim N^\alpha$) in the crossover region between the weak interaction regime with $\alpha = {}^3/_5$ and the chain stretching regime with $\alpha = 1$, when v and κ are held constant in an appropriate manner. The location and the nature of this crossover region can lead to unexpected chain length dependence on the force–distance profiles.

IV. Computational Enumeration

To study the density profile of polyelectrolyte brushes beyond the scaling described in the last section, computational enumeration based upon eqs 2.5 and 2.6 was performed. This section describes the procedure used and the results of this work.

The Hamiltonian of eq 2.5 describes the continuum limit of a one-dimensional random walk, described by $z(s)$; $0 \geq s \geq L$ in the presence of a potential,

$$E[z(s)] = \frac{1}{2}\int_0^L ds \int_0^L ds'\, V[z(s) - z(s')] \qquad (4.1)$$

where V is given by eq 2.5a. By thermal averaging over a large ensemble of randomly generated random walks, the density profile is determined as a function of the variables v, κ, w, and L.

A large number, N, of random walks (typically $N = 10^8$) are generated. Each random walk begins at the surface and consists of N randomly chosen unit steps ($l = 1$). The location after each step is designated z_i for $i = 1, N$, with the first step $z_1 = 1$. Since each step is a random unit length step, z_i is an integer. Absorbing boundary conditions[31,32] are enforced by discarding configurations which intersect the wall; any chain with $z_i = 0$ for any $i > 1$ is thrown out. For each configuration generated, the density is calculated:

$$\varrho(z) = \sum_{i=1}^{N} \delta_{z,z_i} \qquad (4.2)$$

In this discrete model both z and z_i are integers.

For each configuration generated, the Boltzmann weight is determined from the following discretized version of the energy term in eq 2.5,

$$E[\{z_i\}] = \frac{1}{2}\sum_i \sum_j V[z_i - z_j] = \frac{1}{2}\sum_z \sum_{z'} \varrho(z)\, V[z - z']\, \varrho(z') \qquad (4.3)$$

with

$$V[z_i - z_j] = w\delta_{z_i,z_j} + \frac{v}{\kappa l}\exp(-\kappa|z_i - z_j|) \qquad (4.3a)$$

The density is then determined by averaging over the ensemble of N random walks,

$$\langle\varrho(z)\rangle = Z^{-1}\sum_{\{z_i\}} \varrho(z)\, e^{-E[\{z_i\}]} \qquad (4.4)$$

with

$$Z \equiv \sum_{\{z_i\}} e^{-E[\{z_i\}]} \qquad (4.4a)$$

Here, the summations are over the N random walks. Since N is large, this sum approximates an exact enumeration. Using this technique, one must be careful to ensure that the ensemble of random walk configurations generated is large enough to contain configurations near the free energy minimum. If the interaction energy is small then relatively few chains are needed to determine the brush density accurately. If, however, the interaction energy is large, then a relatively large number of configurations must be generated in order to accurately determine the brush density. To illustrate this point, if the limiting case of very strong interaction energy is considered (i.e. the $T \to 0$ limit), the result of Boltzmann weighting is that only the fully streched random walk contributes to any thermodynamic average. In this case, in order to accurately determine the brush density profile, the number of random walk chains generated should be on the order of 2^N.

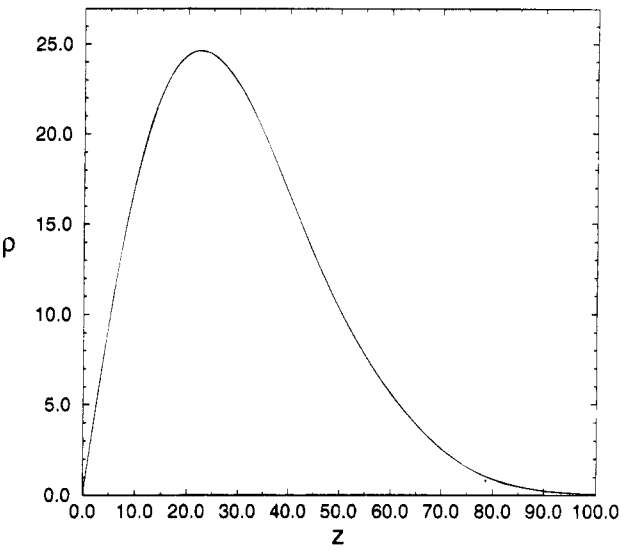

Figure 3. Gaussian brush density profile for $N = 1024$, $l = 1$.

This procedure is used to determine the density profile of polyelectrolyte brushes for a wide range of parameters which will now be discussed.

If both the short-ranged self-excluding and long-ranged electrostatic interactions are absent ($v = w = 0$), then the brush is Gaussian. Figure 3 shows the density profile $\varrho(z)$ for such a brush. The brush shown contains 1024 steps, and z is measured in units of l. This density profile is exactly the same as the analytical result (see ref 3).

The thickness, d, of the brush is obtained graphically from Figure 3. The value of z where the density drops to half the maximum value was used as the measure of brush height, d. When the self-interaction is strong, there may not be a well-defined maximum in the density profile; typically, a large plateau region exists (see, for example, Figure 7). In this case, d is taken to be the value of z where the density is half the density in the plateau region. An alternative measure of the brush height is the root-mean-square (RMS) of the density distribution, $d_{RMS} = (\sum_z z^2\, \varrho(z)/\sum_z \varrho(z))^{1/2}$ which has the same scaling behavior as d. Although d_{RMS} is easier to compute than d, we have chosen d as a measure of brush height because it may be more practical for comparison with experimental observation.

After repeating the enumeration for different values of N and determining d, the N dependence of d is presented in Figure 4 where $d/lN^{1/2}$ is plotted double logarithmically against N. It is clear from Figure 4 that $d \sim N^{1/2}$ in this limit, as expected from eq 3.7.

If $w = 0$, but the electrostatic interaction parameter, $vN^{5/2}$, is sufficiently large, the brush height depends upon $\kappa lN^{1/2}$. Figures 5–7 show the density profiles of polyelectrolyte brushes over a range of κ. When $\kappa lN^{1/2}$ is large (i.e. strong screening by counterions), the brush is effectively Gaussian with brush height proportional to $lN^{1/2}$. As $\kappa lN^{1/2}$ is lowered (i.e. screening is decreased), the height of the brush increases. In this regime, the brush height dependence on $\kappa lN^{1/2}$ varies with $vN^{5/2}$: if $vN^{5/2}$ is large, the dependence is strong; if $vN^{5/2}$ is small, the dependence is weak. This is shown in Figure 8, which is a double logarithmic plot of d vs κ for different values of v. If $vN^{5/2}$ is sufficiently large, as $\kappa lN^{1/2}$ is decreased, eventually the brush becomes fully stretched. At this point $d \approx lN$ and further stretching is not possible. Although this effect is not predicted by the

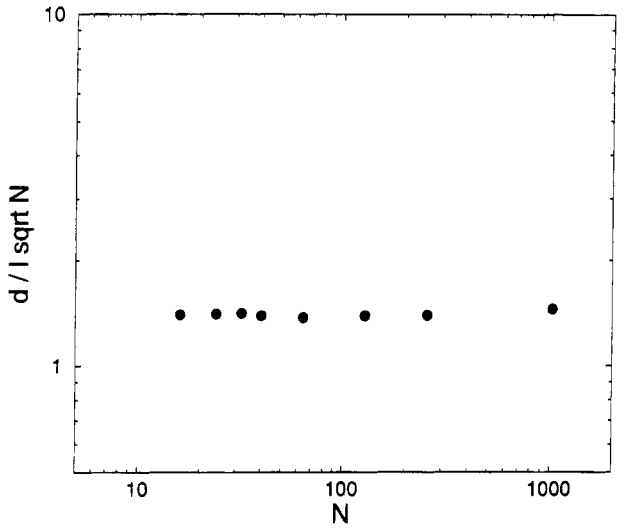

Figure 4. Gaussian brush height dependence on N.

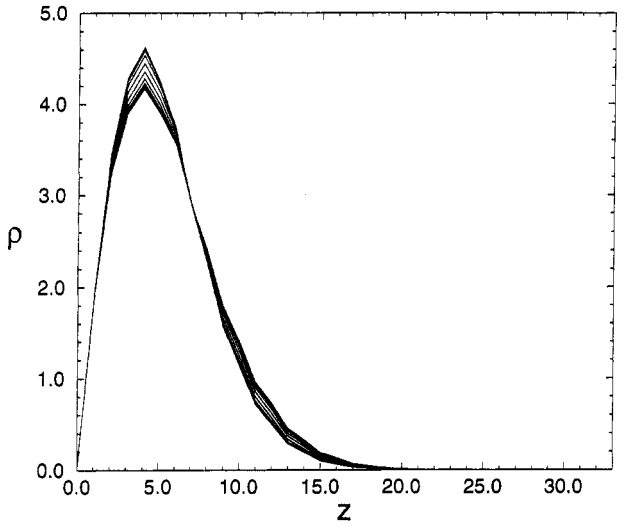

Figure 5. Polyelectrolyte brush density profile for $N = 32$, $l = 1$, $v = 0.000\,488\,28$. The least stretched case is for $\kappa = 4$. Each subsequent curve is a factor of 2 decrease in κ.

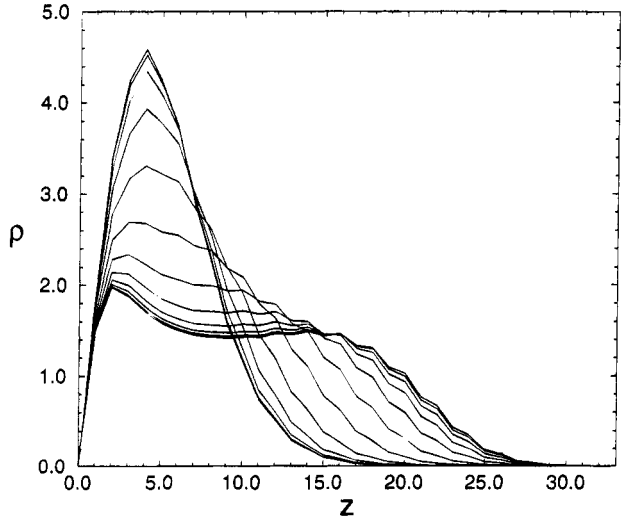

Figure 6. Polyelectrolyte brush density profile for $N = 32$, $l = 1$, $v = 0.003\,906\,25$. The least stretched case is for $\kappa = 4$. Each subsequent curve is a factor of 2 decrease in κ.

continuous Hamiltonian (eq 2.5), the enumeration uses a discretized model with a finite number of steps, and therefore considers chains which are finitely extensible.

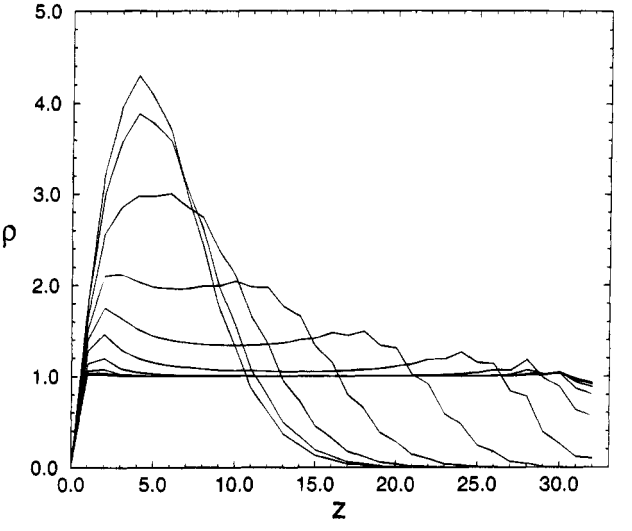

Figure 7. Polyelectrolyte brush density profile for $N = 32$, $l = 1$, $v = 0.031\,25$. The least stretched case is for $\kappa = 4$. Each subsequent curve is a factor of 2 decrease in κ.

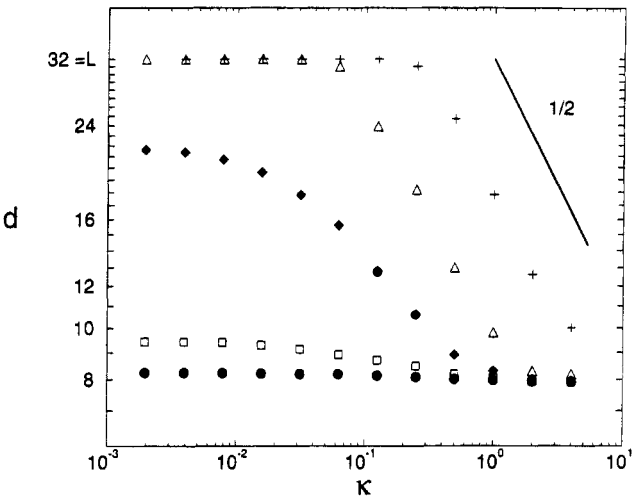

Figure 8. Polyelectrolyte brush height, d, vs κ: (●) $v = 0.000\,244$; (□) $v = 0.000\,977$; (♦) $v = 0.003\,906$; (△) $v = 0.015\,625$; (+) $v = 0.125$. The value of 0.5 for the apparent exponent β is included as a guide to the slope.

Thus, the enumeration captures the physical effect of saturation when $d \to lN$.

Figure 8 shows that the crossover between the stretched brush at small values of κ and the unstretched brush at large values of κ is strongly dependent on the value of $vN^{5/2}$. If $vN^{5/2}$ is sufficiently large, d can depend on κ as an effective power law, $d \sim \kappa^{-\beta}$. This, in turn, gives the brush height dependence on the salt concentration, c_s. For monovalent ions, κ is proportional to $c_s^{1/2}$ and, consequently, $d \sim c_s^{-\beta/2}$. The particular value of β depends on $vN^{5/2}$ and the range of κ. As a guideline to the eye, a slope of $\beta/2 = -0.25$ is included in Figure 8. Similar values for the apparent exponent β have recently been observed experimentally in polyelectrolyte brush systems.[33]

Figures 9–11 show the dependence of brush height upon $vN^{5/2}$ at different values of $\kappa lN^{1/2}$. If $\kappa lN^{1/2}$ is large, and $(\kappa lN^{1/2})^2$ is large compared with $vN^{5/2}$, the brush is Gaussian with size

$$d \sim lN^{1/2} \tag{4.5}$$

This is shown in Figure 9.

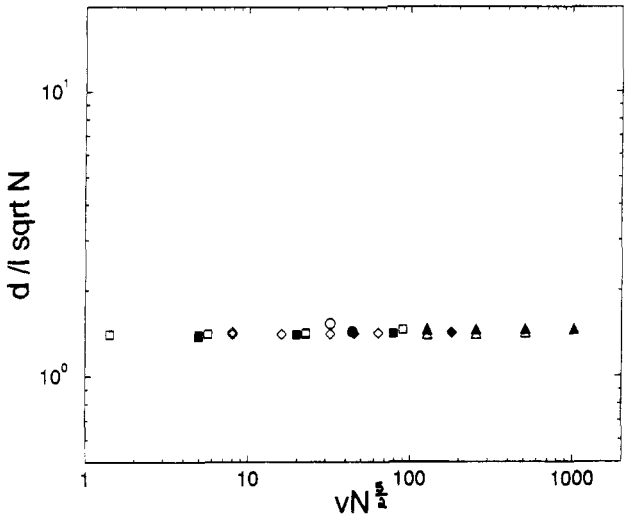

Figure 9. Reduced brush height $d/lN^{1/2}$ vs $vN^{5/2}$: (○) $N = 16$; (●) $N = 24$; (□) $N = 32$; (■) $N = 40$; (◇) $N = 64$. $\kappa lN^{1/2}$ is large but $(\kappa lN^{1/2})^2$ is small compared with $vN^{5/2}$.

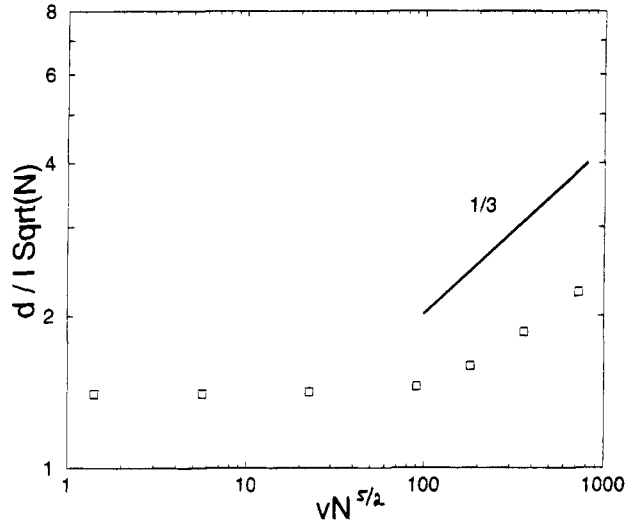

Figure 10. Reduced brush height $d/lN^{1/2}$ vs $vN^{5/2}$. $l = 1$, $N = 32$, $\kappa = 2$. Crossover from Gaussian behavior to $^1/_3$ power law when $vN^{5/2}$ becomes large compared with $(\kappa lN^{1/2})^2$. A slope of $^1/_3$ is included as a guide.

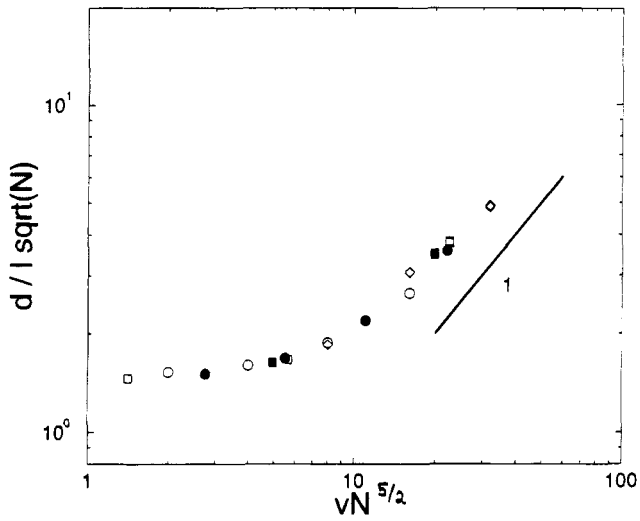

Figure 11. Reduced brush height $d/lN^{1/2}$ vs $vN^{5/2}$: (○) $N = 16$; (●) $N = 24$; (□) $N = 32$; (■) $N = 40$; (◇) $N = 64$. $0.78 < \kappa lN^{1/2} < 0.031\,26$, $d/lN < 0.9$. A slope of 1 is included as a guide.

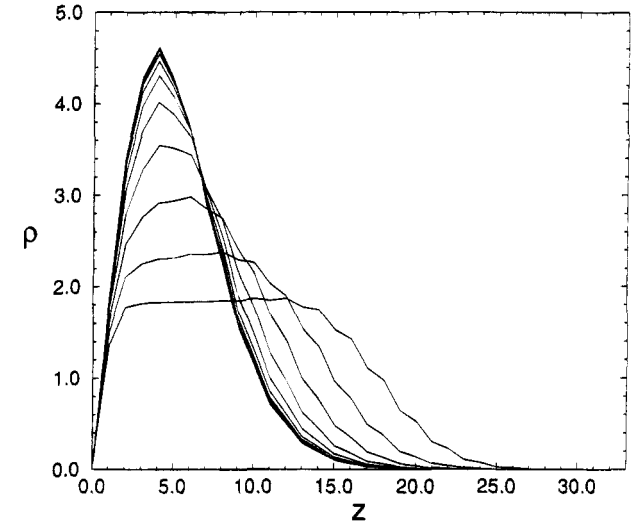

Figure 12. Self-excluding brush density profile. $L = 32$. The most stretched profile is for $w = 0.250$. Each subsequent curve is for a factor 2 decrease in w.

If $\kappa lN^{1/2}$ is large, but $(\kappa lN^{1/2})^2$ is small compared with $vN^{5/2}$, then the brush height dependence on $vN^{5/2}$ (for fixed $\kappa lN^{1/2}$) is $lN^{1/2}(vN^{5/2})^{1/3}$ (see Figure 10). In this regime, the electrostatic interaction is effectively short-ranged with strength $v/\kappa^2 l^2$ and

$$d \sim v^{1/3}\kappa^{-2/3}l^{1/3}N \tag{4.6}$$

as expected from eq 3.13.

Finally, if $\kappa lN^{1/2}$ is small and $vN^{5/2}$ is sufficiently large,

$$d \sim vN^3 \tag{4.7}$$

as predicted by eq 3.9. This is shown in Figure 10.

For reference, we consider the effect of a short-ranged interaction only (i.e. $v = 0$). Figure 12 shows the effect of changing the strength of the interaction parameter, w, on the density profile of a self-excluding brush. At low values of w, the brush is effectively Gaussian, with $d \sim lN^{1/2}$; at larger values of w, $d \sim w^{1/3}lN^{1/2}$. As with the long-ranged electrostatic interaction, saturation occurs when $d \approx lN$.

V. Variational Procedure

The key conclusions of the enumeration results for the recovery of scaling laws and their crossovers can be obtained by a variational approach. This technique, which is successful in determining the size of a polyelectrolyte chain in a bulk salt solution, can be applied directly to the one-dimensional Hamiltonian given by eq 2.5. The result of this approach is that the charged chain may be approximated by a Gaussian chain with an effective Kuhn length l_{eff} which depends upon q, κ, w, and L (=Nl). The average size of such a chain (i.e. radius of gyration), is, therefore, $(l_{\text{eff}}L/6)^{1/2}$. This method may be applied immediately to the one-dimensional Hamiltonian (eq 2.5) of the brush problem. When this procedure is applied (see ref 30 for details), l_{eff} satisfies the following relationship:

$$l_{\text{eff}}^{1/2}\left(\frac{1}{l} - \frac{1}{l_{\text{eff}}}\right) = \zeta_{\text{se}} + \zeta_{\text{sc}} \tag{5.1}$$

with the self-excluding part

$$\zeta_{\text{se}} = \frac{2^{3/2}wL^{3/2}}{15\pi^{1/2}ll_{\text{eff}}} \tag{5.1a}$$

and the screened Coulombic part

$$\zeta_{sc} = \frac{2^{3/2} v L^{5/2}}{\pi^{1/2} l^3}\left(\frac{\pi^{1/2}}{2}(a^{-3/2} - 4a^{-5/2} + 6a^{-7/2})e^a \times \right.$$
$$\left. \mathrm{erfc}(a^{1/2}) + 3\pi^{1/2}a^{-7/2} - 6a^{-3} + \pi^{1/2}a^{-5/2} + \frac{a^{-1}}{15}\right) \quad (5.1b)$$

with

$$a \equiv \frac{\kappa^2 l_{\mathrm{eff}} L}{2} \quad (5.1c)$$

Here, we use L ($=lN$) in order to retain notation consistent with the similar calculation for the bulk polelectrolyte (see ref 30). In the limit of $q^2 \to 0$ (i.e. self-excluded volume effect only), this reduces to the following relationship between l_{eff} and l:

$$l_{\mathrm{eff}}^{1/2}\left(\frac{l_{\mathrm{eff}}}{l} - 1\right) = \frac{2^{3/2} w L^{3/2}}{15\pi^{1/2} l} \quad (5.2)$$

This describes the crossover between $l_{\mathrm{eff}} \sim l$ for $wN^{3/2} \ll 1$ and $l_{\mathrm{eff}} \sim w^{2/3}L$ for $wN^{3/2} \gg 1$.

In the limit that only electrostatic self-interactions are considered (i.e. $vL^{5/2} \gg wL^{3/2}$), the limits of eq 3.4 are

$$l^{1/2}{}_{\mathrm{eff}}\left(\frac{1}{l} - \frac{1}{l_{\mathrm{eff}}}\right) = \frac{2^{3/2} v L^{5/2}}{\pi l^3}\begin{cases}\frac{2}{35} & \kappa \to 0 \\ \frac{2}{15\kappa^2 l_{\mathrm{eff}} L} & \kappa\sqrt{\frac{l_{\mathrm{eff}} L}{2}} \to \infty\end{cases} \quad (5.3)$$

This formula describes the crossover between $l_{\mathrm{eff}} \sim v^2 N^5 l$ for $\kappa \to 0$ and $l_{\mathrm{eff}} \sim (v/\kappa^2 l^2)^{2/3} L$ for $\kappa(l_{\mathrm{eff}}L/2)^{1/2} \gg 1$. Therefore, the polyelectrolyte brush problem is approximated by considering a Gaussian chain with one end located at the surface and an effective Kuhn length, l_{eff}, which is determined self-consistently from eqs 5.1–5.3. The configurational properties of Gaussian chains near surfaces are well-known.[31,32] The size of a Gaussian brush with the appropriate boundary condition at the surface is proportional to $l_{\mathrm{eff}}^{1/2}$:[32]

$$d \approx \sqrt{2} l_{\mathrm{eff}}^{1/2} L^{1/2} \quad (5.4)$$

This value corresponds to the RMS end point height of the brush, which is, to within a small numerical factor, the brush height we have used in the previous section. Therefore, the combination of eqs 5.4 and 5.2 yields for the case of $vN^{5/2} \ll wN^{3/2}$

$$d \sim \begin{cases} lN^{1/2} & wN^{3/2} \ll 1 \\ w^{1/3} lN & wN^{3/2} \gg 1 \end{cases} \quad (5.5)$$

Also, the combination of eqs 5.4 and 5.3 gives for the case of $wN^{3/2} \ll vN^{5/2}$,

$$d \sim \begin{cases} vlN^3 & \kappa lN^{1/2} \to 0 \\ \left(\frac{v}{\kappa^2 l^2}\right)^{1/3} lN & \kappa d \gg 1 \end{cases} \quad (5.6)$$

These laws are, in fact, the same as the scaling laws derived in section III at the appropriate conditions. The crossover between the various asymptotic results is completely described by eqs 5.1 and 5.4.

Figure 12 shows the dependence of $(l_{\mathrm{eff}}/l)^{1/2}$ (which is proportional to the "reduced" brush size, $d/lN^{1/2}$) upon the interaction strength variable $vN^{5/2}$ at different values of the screening strength variable $\kappa lN^{1/2}$. The different regimes described earlier are evident. At very low values of $vN^{5/2}$ (i.e., low charge density on the brush), the brush is essentially Gaussian with $l_{\mathrm{eff}} = l$ so that $d \sim lN^{1/2}$. At very large values of $vN^{5/2}$, $l_{\mathrm{eff}}^{1/2} \sim l^{1/2}(vN^{5/2})^{1/3} f(\kappa lN^{1/2})$ with the proportionality factor f being a decreasing function of $\kappa lN^{1/2}$. In fact, this function $f(\kappa lN^{1/2})$ is proportional to $(\kappa lN^{1/2})^{-2/3}$ for large values of $\kappa lN^{1/2}$. Therefore, at fixed values of $\kappa lN^{1/2}$, $d \sim (l_{\mathrm{eff}} lN)^{1/2} \sim lN^{1/2}(vN^{5/2})^{1/3} f(\kappa lN^{1/2})$ in this limit. Between these extremes is a regime where the size of the polyelectrolyte brush is strongly determined by the value of the screening strength variable $\kappa lN^{1/2}$: in this regime, the brush size (for fixed $\kappa lN^{1/2}$) can be written as

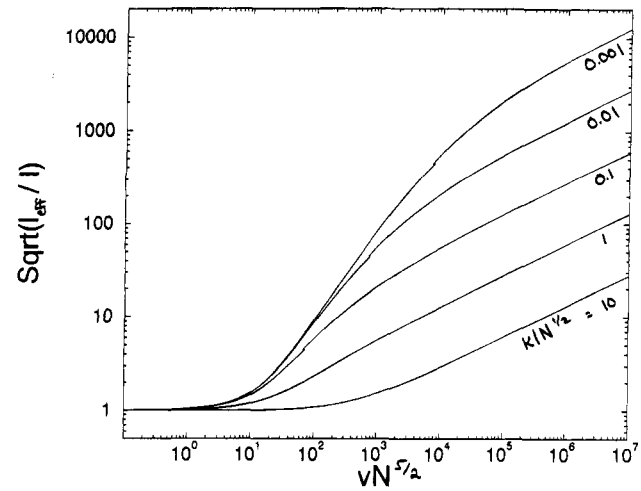

Figure 13. $(l_{\mathrm{eff}}/l)^{1/2}$ vs $vN^{5/2}$ for several values of $\kappa lN^{1/2}$. The bottom curve is for $\kappa lN^{1/2} = 10$. Each subsequent curve is for a factor 10 decrease in $\kappa lN^{1/2}$.

$$d \sim l_{\mathrm{eff}} N^{1/2} \sim lN^{1/2}(vN^{5/2})^x f(\kappa lN^{1/2}) \quad (5.7)$$

with x having the following limits:

$$^1/_3 < x < 1 \qquad x = \begin{cases} 1 & \kappa lN^{1/2} \to 0 \\ ^1/_3 & \kappa lN^{1/2} \to \text{large} \end{cases} \quad (5.8)$$

In the large $\kappa lN^{1/2}$ limit, $d \sim v^{1/3}\kappa^{-2/3} l^{1/3} N$ after using the asymptotic form of f, as discussed above. The variational approach used predicts the crossover observed by computational enumeration. Comparison of Figures 11 and 13 shows fairly good agreement in the onset of brush height increase with interaction strength, $vN^{5/2}$.

VI. Conclusions and Discussion

We have identified the dimensionless variables to describe the effect of both the short-ranged van der Waals interaction and the long-ranged electrostatic interaction on the properties of the polyelectrolyte brushes. The parameter accounting for the short-ranged interaction is $wN^{3/2}$. w is proportional to the product of the grafting density, σ, and the usual excluded volume parameter, $\bar{w}$. Two dimensionless parameters, $vN^{5/2}$ and $\kappa lN^{1/2}$ describe the long-ranged electrostatic interaction. The strength v is $2\pi\sigma q^2 e^2 l^3/\epsilon k_B T$ where q is the number of charges per Kuhn length on the polyelectrolyte backbone. κ is the inverse Debye screening length.

On the basis of scaling, computational enumeration, and variational calculations, we have obtained a number of important features of polyelectrolyte brush density profiles:

(1) Brush Height Dependence on $vN^{5/2}$ and $\kappa lN^{1/2}$. In general, there are four regimes. In the first regime, with weak grafting density, brush height is proportional to N^{ν} with the effective exponent ν varying between $^1/_2$ and $^3/_5$ depending on the strength of w. As $vN^{5/2}$ increases, the second regime with $d \sim vlN^3$ emerges if $\kappa lN^{1/2}$ is sufficiently small (low salt concentration) and $vN^{5/2}$ is sufficiently large. If $\kappa lN^{1/2}$ is increased from this regime, the exponent 3 decreases. The third regime corresponds to the situation of high salt concentration $\kappa lN^{1/2} \gg 1$, when the electrostatic interaction is essentially short-ranged and the grafting density is sufficiently high. In this regime, the chain is stretched with the strength of stretching in accordance with $d \sim (w + (2v/\kappa^2 l^2))^{1/3} lN$. In this case, the problem reduces to a one-dimensional walk problem. The fourth regime corresponds to full chain stretching, $d \approx lN$ for larger values of v and w.

The boundaries of the three regions and the crossover ranges are given in Figure 1. The same results can be presented in an alternative way. If $\kappa lN^{1/2}$ is held fixed, the reduced brush height, $d/lN^{1/2}$, scales as a power of $vN^{5/2}$ between 0 and 1, as shown in Figures 9–11. If both $\kappa lN^{1/2}$ and $vN^{5/2}$ are large, then the scaling behavior of brush height depends on $vN^{3/2}/\kappa^2 l^2$: if $vN^{3/2}/\kappa^2 l^2$ is small, $d \sim lN^{\nu}$; if $vN^{3/2}/\kappa^2 l^2$ is large, $d \sim (w + (2v/\kappa^2 l^2))^{1/3} lN$. At fixed $vN^{5/2}$ (fixed charge density and grafting density), computational enumeration shows (see Figure 8) the effect of $\kappa lN^{1/2}$ (i.e. varying the salt concentration of monovalent ions) on d. The brush height decreases with an increase in the salt concentration. This is in qualitative agreement with the experimental observation of decreases in interaction ranges with salt concentration when two polyelectrolyte brushes are brought closer.

(2) Brush Density Shape. The computational enumeration shows, in detail, the shape of a polyelectrolyte brush density profile (see Figures 5–7). The density profiles determined by computational enumeration are more complex than either the step function used in the Alexander–de Gennes approach[4,5] or the profiles predicted by the mean-field approach of Zhulina *et al.* and Milner *et al.*[6,7] At the wall ($z = 0$), the brush density is zero. In the other descriptions, this feature is absent. In the Alexander–de Gennes approach a step function is assumed; in the treatment of this problem by Milner *et al.*, absorbing boundary conditions are not imposed.

Additionally, computational enumeration includes the effect of fluctuations which are neglected in mean-field treatments of this problem. For comparison, if only the short-ranged, self-excluding interaction is considered (i.e. $v = 0$), the approach of Milner *et al.* predicts a parabolic density profile. Computational enumeration describes a density profile which is roughly parabolic, but with a somewhat exponentially decaying tail. This is consistent with neutron scattering measurements.[18] It should also be noted that in the $T \to 0$ limit (i.e. strong interaction limit) the density profile approaches the step-function profile used in the Alexander–de Gennes treatments.

The shape of the polyelectrolyte brush ($v \neq 0$) is more complicated than the self-excluding brush. Near the $T \to 0$ limit, the shape of the polyelectrolyte brush is roughly a step function but with a greater density in the region $z \approx d$ than in the case of a self-excluding brush. This is due to the fact that density excesses are energetically favorable at the extremes (rather than in the region near $z = d/2$). For short-ranged interactions, there is no energy associated with the location of density excesses and this effect does not exist. This effect underlies the difference between the density profiles of long-ranged, electrostatically interacting brushes and those with a short-ranged interaction. This effect becomes less pronounced as the range of the electrostatic interaction, κ^{-1}, is decreased. Since a short-ranged interaction potential is the limiting case (i.e. the $\kappa \to \infty$ limit) of the screened Coulombic potential, it is clear that as κ becomes large, the polyelectrolyte brush density profile approaches that of a self-excluding brush.

(3) Finite Extensibility. Finite extensibility is a natural consequence of the model used in computational enumeration. The Hamiltonians of the approach used by Milner *et al.* and the model Hamiltonians of section II are continuum idealizations of the random walk when the polymer chains are not strongly stretched. These models are infinitely extensible. Therefore they do not capture the physical effect of saturation when the brush is strongly stretched. Recently, in order to describe this saturation, Shim and Cates include this effect using the method of Milner *et al.* by a modification of the free energy term.[9]

The application of a variational approximation to this problem predicts the size of the polyelectrolyte brush. The accuracy of this technique should be best when the brush is not strongly stretched. While this approach ignores the effect of boundary conditions imposed at the surface, it yields analytical brush size predictions which are consistent with the results of computational enumeration.

The use of a screened Coulombic interaction potential is valid when the local potential is not large and the size of counterions is small compared with the screening length, κ^{-1}. Recently, the structure of polyelectrolytes has been studied by simulation.[34] This work suggests that at large charge densities the interaction potential deviates from the screened Coulombic potential used here. While the use of a screened Coulombic potential is certainly accurate for low charge densities, this approach fails to consider the presence of charges due to the polyelectrolyte itself and therefore loses its applicability at high charge densities. Typically, the value of κ which is calculated using Debye–Hückel theory (see eq 2.1), only accounts for counterions due to added salt. To develop a more precise theory of charged brushes, a more complete theory of screening is needed to properly account for local changes in screening due to all charges in the system.

The extension of this work to a number of useful areas is possible. For example, Ross and Pincus have predicted the phase transitions of a polyelectrolyte brush in a poor solvent (i.e. $w < 0$, $v \neq 0$). Also, an understanding of the stabilization forces between colloidal particles with grafted polyelectrolytes may be developed from this work.

Acknowledgment. We are grateful to Professor M. Tirrell for stimulating discussions and for bringing ref 23 to our attention. Acknowledgment is made to the NSF grant DMR 9221146001 and to the Materials Research Laboratory at the University of Massachusetts.

References and Notes

(1) Napper, D. H. *Polymeric stabilization of colloidal dispersions*; Academic: New York, 1983.
(2) Isrealachvilli, J. *Intermolecular and surface forces with applications to colloidal and biological systems*; Academic: London, 1985.
(3) Dolan, A. K.; Edwards, S. F. *Proc. R. Soc. London, Ser. A* **1974**, *337*, 509.
(4) de Gennes, P. G. *Macromolecules* **1980**, *13*, 1069.
(5) Alexander, S. *J. Phys. Paris* **1977**, *38*, 983.
(6) Milner, S. T.; Witten, T. A.; Cates, M. E. *Macromolecules* **1988**, *21*, 2610.
(7) Zhulina, E.; Borisov, O.; Priamitsyn, V. *J. Colloid Interface Sci.* **1990**, *137*, 495.
(8) Muthukumar, M.; Ho, J. *Macromolecules* **1989**, *22*, 965.
(9) Shim, D. F. K.; Cates, M. E. *J. Phys. Paris* **1989**, *50*, 3535.
(10) Wijmans, C. M.; Scheutjens, J. M. H. M.; Zhulina, E. B. *Macromolecules* **1992**, *25*, 2657.
(11) Carignano, M. A.; Szleifer, I. *J. Chem. Phys.* **1993**, *98*, 5006. Carignano, M. A.; Szleifer, I. *J. Chem. Phys.* **1994**, *100*, 3210. Carignano, M. A.; Szleifer, I. *Macromolecules* **1994**, *27*, 702.
(12) Cosgrove, T.; Heath, T.; van Lent, B.; Leermakers, F.; Scheutjens, J. *Macromolecules* **1987**, *20*, 1692.
(13) Grest, G.; Murat, M. *Macromolecules* **1993**, *26*, 3108. Murat, M.; Grest, G. S. *Macromolecules* **1991**, *24*, 704. Murat, M.; Grest, G. S. *Macromolecules* **1989**, *22*, 4054.
(14) Chakrabarti, A.; Toral, R. *Macromolecules* **1990**, *23*, 2016.
(15) Hadziioannou, G.; Patel, S.; Granick, S.; Tirrell, M. *J. Am. Chem. Soc.* **1986**, *108*, 2869.
(16) Taunton, H. J.; Toprakcioglu, C.; Fetters, L. J.; Klein, J. *Macromolecules* **1990**, *23*, 571.
(17) Field, J. B.; Toprakcioglu, C.; Ball, R. C.; Stanley, H. B.; Dai, L.; Barford, W.; Penfold, J.; Smith, G.; Hamilton, W. *Macromolecules* **1992**, *25*, 434.
(18) Auroy, P.; Auvray, L.; Leger, L. *Physica A* **1991**, *172*, 269. Auroy, P.; Mir, Y.; Auvray, L. *Phys. Rev. Lett.* **1992**, *69*, 93.
(19) Halperin, A.; Tirrell, M.; Lodge, T. P. *Adv. Polym. Sci.* **1991**, *100*, 1992.
(20) Milner, S. *Science* **1991**, *251*, 905.
(21) Miklavic, S. J.; Marcelja, S. *J. Phys. Chem.* **1988**, *92*, 6718.
(22) Misra, S.; Varanasi, S.; Varanasi, P. P. *Macromolecules* **1989**, *22*, 4173.
(23) Pincus, P. *Macromolecules* **1991**, *24*, 2912.
(24) Ross, R. S.; Pincus, P. *Macromolecules* **1992**, *25*, 2177.
(25) Borisov, O. V.; Birshtein, T. M.; Zhulina, E. B. *J. Phys. II* **1991**, *1*, 521.
(26) Zhulina, E. B.; Borisov, O. V.; Birshtein, T. M. *J. Phys. II* **1992**, *2*, 63.
(27) Borisov, O. V.; Zhulina, E. B.; Birshtein, T. M. *Macromolecules* **1994**, *27*, 4795.
(28) See, for example: Doi, M.; Edwards, S. F. *The Theory of Polymer Dynamics*; Oxford University Press: Oxford, U.K., 1986; Chapter 2.
(29) Weigel, F. W. *J. Phys. A* **1977**, *10*, 299.
(30) Muthukumar, M. *J. Chem. Phys.* **1987**, *86*, 7230.
(31) Chandrasekar, S. *Rev. Mod. Phys.* **1943**, *15*, 3.
(32) Lepine, Y.; Caille, A. *Can. J. Phys.* **19**, *56*, 403. Eisenriegler, E.; Kremer, K.; Binder, K. *J. Chem. Phys.* **1982**, *77*, 6296.
(33) Watanabe, H.; Patel, S. S.; Argillier, J. F.; Parsonage, E. E.; Mays, J.; Dan-Brandon, N.; Tirrell, M. *Mater. Res. Soc. Proc.* **1992**, *249*, 255.
(34) Stevens, M.; Kremer, K. *Phys. Rev. Lett.* **1993**, *71*, 2228. Stevens, M.; Kremer, K. *Macromolecules* **1993**, *26*, 4717.

MA9501104